

This is an Open Access document downloaded from ORCA, Cardiff University's institutional repository:<https://orca.cardiff.ac.uk/id/eprint/111006/>

This is the author's version of a work that was submitted to / accepted for publication.

Citation for final published version:

Anyah, R.O., Forootan, E. , Awange, J.L. and Khaki, M. 2018. Understanding linkages between global climate indices and terrestrial water storage changes over Africa using GRACE products. *Science of the Total Environment* 635 , pp. 1405-1416. 10.1016/j.scitotenv.2018.04.159

Publishers page: <http://dx.doi.org/10.1016/j.scitotenv.2018.04.159>

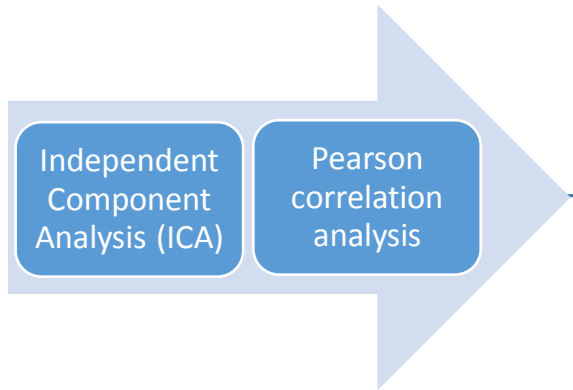
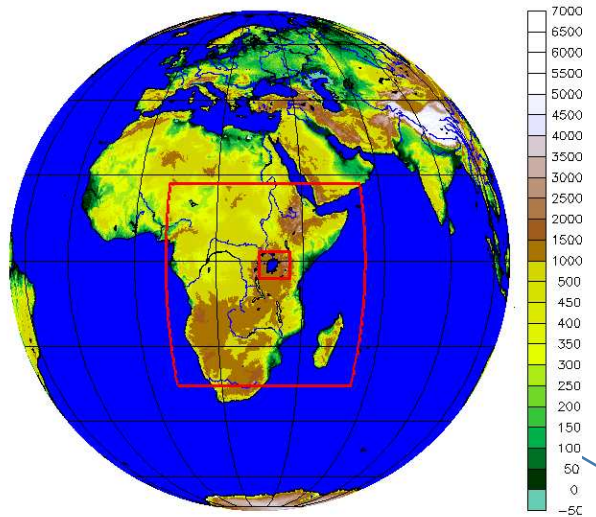
Please note:

Changes made as a result of publishing processes such as copy-editing, formatting and page numbers may not be reflected in this version. For the definitive version of this publication, please refer to the published source. You are advised to consult the publisher's version if you wish to cite this paper.

This version is being made available in accordance with publisher policies. See <http://orca.cf.ac.uk/policies.html> for usage policies. Copyright and moral rights for publications made available in ORCA are retained by the copyright holders.



Gravity Recovery And Climate Experiment (GRACE) Terrestrial Water Storage (TWS)



- Indian Ocean Dipole (IOD)
- Quasi-Biennial Oscillation (QBO)
- Madden-Julian Oscillation (MJO)
- North Atlantic Oscillation (NAO)
- El Niño-Southern Oscillation (ENSO)

The first dominant Independent Components (IC) are linked to NAO, and are characterized by significant reductions of TWS over southern Africa

The second dominant ICs are associated with IOD and are characterized by significant increases in TWS over equatorial eastern Africa

The combined ENSO and MJO are apparently linked to the third ICs, which are also associated with significant increase in TWS changes over both southern Africa as well as equatorial eastern Africa

Research highlights:

- Connections between global climate-teleconnections and TWS changes were investigated
- We found regions where climate indices (CI) and TWS relationships were very strong
- Climate indices in some areas largely influence TWS spatiotemporal variabilities
- NAO was highly correlated with the leading ICA mode over parts of southern Africa
- Lagged correlations between the ICA mode and TWS were stronger over southern Africa

1 **Understanding linkages between global climate indices and terrestrial water storage**
2 **changes over Africa using GRACE products**

3 R.O. Anyah^a, E. Forootan^{b,c}, J.L. Awange^b, M. Khaki^b

4
5 ^a*Dept. of Natural Resources and the Environment, University of Connecticut, USA*

6 ^b*School of Earth and Planetary Sciences, Discipline of Spatial Sciences, Curtin University,*
7 *Perth, Australia.*

8 ^c*Geodetic Institute, Karlsruhe Institute of Technology, Karlsruhe, Germany*

9

10 **Abstract**

11 Africa, a continent endowed with huge water resources that sustain its agricultural activities is
12 increasingly coming under threat from impacts of climate extremes (droughts and floods), which
13 puts the very precious water resource into jeopardy. Understanding the relationship between
14 climate variability and water storage over the continent, therefore, is paramount in order to
15 inform future water management strategies. This study employs Gravity Recovery And Climate
16 Experiment (GRACE) satellite products and the higher order (fourth order cumulant) statistical
17 independent component analysis (ICA) method to study the relationship between Terrestrial
18 Water Storage (TWS) changes and five global climate-teleconnection indices; El Niño-Southern
19 Oscillation (ENSO), North Atlantic Oscillation (NAO), Madden-Julian Oscillation (MJO),
20 Quasi-Biennial Oscillation (QBO) and the Indian Ocean Dipole (IOD) over Africa for the period
21 2003-2014. Pearson correlation analysis is applied to extract the connections between these
22 climate indices (CIs) and TWS, from which some known strong CI-rainfall relationships (e.g.,
23 over equatorial eastern Africa) are found. Results indicate *unique linear-relationships* and
24 *regions* that exhibit strong linkages between CIs and TWS. Moreover, unique regions having
25 strong CI-TWS connections that are completely different from the typical ENSO-rainfall
26 connections over eastern and southern Africa are also identified. Furthermore, the results indicate
27 that the first dominant Independent Components (IC) of the CIs are linked to NAO, and are
28 characterized by significant reductions of TWS over southern Africa. The second dominant ICs
29 are associated with IOD and are characterized by significant increases in TWS over equatorial
30 eastern Africa, while the combined ENSO and MJO are apparently linked to the third ICs, which
31 are also associated with significant increase in TWS changes over both southern Africa as well
32 as equatorial eastern Africa.

33

34 **Keywords:**

35 Africa, Terrestrial Water Storage (TWS), Climate Indices, GRACE, ENSO, IOD, NAO, MJO,
36 QBO, Climate-TWS Hotspots

37

38 **1.0 Introduction**

39 Africa (Figure 1), the world's poorest continent faces myriad of climate-related extremes, e.g.,
40 droughts and floods (see, e.g., Lyon et al., 2014, Omondi et al., 2014, Awange et al., 2016a,
41 Mpelesoka et al., 2017, Ndehedehe et al., 2018), which fuel food insecurity thereby putting
42 millions of lives at risk (e.g., Agutu et al., 2017). Given the large dependency of the continent on

43 rain-fed agriculture (Agola and Awange 2015, Agutu et al., 2017), understanding the relationship
44 that exists between Terrestrial Water Storage (TWS; i.e., a summation of soil moisture,
45 groundwater, surface, and vegetation water storage compartments) and global climate
46 teleconnection indices is essential for agricultural production on the one hand, and for improving
47 the understanding of interactions between climate variability (through, e.g., climate indices) and
48 the water cycle on the other hand. This is also important for managing the water resources in arid
49 and semi-arid regions of the continent, and for the general planning purposes in order to make
50 the continent food secure. Whereas the relationships between climate indices and rainfall is
51 relevant for meteorological drought mitigation (e.g., Clark et al., 2003, Naumann et al., 2014,
52 Kurnik et al., 2011, Awange et al., 2016a, 2016b, and Mpelesoka et al., 2017), it is also vital to
53 understand the relationship between climate indices and TWS in order to be able to mitigate both
54 hydrological drought as well as agricultural droughts (e.g., Anderson et al., 2012; AghaKouchak,
55 2015).

56
57 The relationships between the global climate teleconnection indices and TWS over Africa can be
58 understood within the context of the general climatology since the drivers of climatological-
59 rainfall patterns over the continent also influence terrestrial water storage recharge in the soil,
60 surface and groundwater reservoirs. The drivers of the general climate (hydroclimate) of Africa
61 are dominated by atmospheric circulation systems (e.g., monsoonal trade winds) and land surface
62 processes, which influence inter-tropical convergence zone (ITCZ), where these winds (and rain-
63 generating moisture) normally converge and affect rainfall patterns. The ITCZ over the African
64 continent has a north-south migration pattern dictated by the position of the overhead sun and
65 tend to influence the location of maximum precipitation, with approximately 3-4 weeks lag time
66 (see e.g., Nicholson, 1996).

67
68 Seasonal rainfall distribution over areas south of the Sahara (see Figure 1) is particularly linked
69 to the movement and position of the ITCZ. However, over the equatorial regions, rainfall tends
70 to be evenly distributed throughout the year (i.e., showing limited dependence on the ITCZ). For
71 higher latitudes, however, especially over the Sahel, rainfall tends to be confined to the summer
72 months-June-September (e.g., Ndehedehe et al., 2016). Over equatorial eastern Africa, rainfall
73 tends to be highly influenced and dictated by southeast and northeast monsoons, depending on
74 the north-south migration of the ITCZ position. Southern African rainfall, on the other hand,
75 tends to exhibit spatio-temporal rainfall distribution largely influenced by major circulation
76 features of the southern hemisphere. For example, from the equator to about 20°S, seasonal
77 rainfall variability tend to be in synch with the movement of the ITCZ whereas the more sub-
78 tropical regions are influenced by semi-permanent high-pressure cells of the general circulation
79 of the atmosphere, characterized by a high degree of intra- and inter-annual variability (Tyson,
80 1986).

81
82 In general, as whole, apparent linkages exist between the global climate indices and rainfall and
83 to an extent with TWS over a number of regions in sub-Saharan Africa (see, e.g., Ndehedehe et
84 al., 2017a, 2018). It is important to note, however, that there may be several other human-
85 induced factors that may contribute to TWS patterns and changes. For example, at the local
86 scale, the effects of complex terrain (topography) and large inland water bodies could be
87 superimposed on the climatological patterns, leading to unique space-time distribution of rainfall
88 and other hydrological features, including variability and changes in TWS. In addition, other

89 human activities related to water resources management and practices such as dam release
90 procedures and abstraction may also contribute to unique changes in local TWS (e.g., Ndehedehe
91 et al., 2017b).

92

93 Although a number of studies have previously investigated and discussed the relationships
94 between global climate indices and rainfall over the African continent (e.g., Becker et al., 2010;
95 Indeje et al., 2000; Mutai and Ward 2001; Awange et al., 2013), the relationship between some
96 of the dominant global climate teleconnection indices and seasonal/inter-annual variability of
97 TWS has not been extensively investigated, except a few recent studies such as Reager and
98 Famiglietti, (2009), Phillips et al., (2012), Awange et al., (2013), Forootan et al., (2014a) and
99 Ndehedehe et al., (2017a, 2018). However, these studies also focus on separate sub-regions of
100 the continent and thus do not consider the entire continent to provide a more comprehensive
101 understanding of the relationship between the continent's TWS and major global climate
102 teleconnection indices. For instance, Awange et al. (2013) look at the Lake Victoria basin in East
103 Africa while Forootan et al., (2014a) and Ndehedehe et al., (2017a, 2018) consider the West
104 Africa region. The reason for this is largely due to the fact that a comprehensive measurement of
105 the components of TWS (surface water, groundwater, soil moisture, snow/ice and biomass) from
106 the insufficient and unreliable in-situ hydroclimate data remains a big challenge (e.g., Creutzfeldt
107 et al., 2010). TWS comprises all forms of water stored on the surface and in the subsurface of the
108 Earth, which is a major component of the hydrological cycle and is critical in understanding the
109 land surface-atmosphere interactions, and exchanges of moisture and energy.

110

111 Since 2002, however, large-scale TWS has been successfully estimated using the gravity
112 observations of Gravity Recovery And Climate Experiment (GRACE, e.g., Tapley et al., 2004).
113 Nominal monthly GRACE TWS can be derived with an accuracy of ~1 cm with few hundred km
114 spatial resolution. GRACE has been applied globally to study the relationship between climate
115 variability and TWS changes. For example, Phillips et al., (2012) and Ni et al., (2018) examined
116 linkages between ENSO and global TWS over the entire globe. Using monthly GRACE-TWS
117 for the period 2003-2010, Phillips et al., (2012) showed peak correlations between Multivariate
118 ENSO Index (MEI) and the measured (GRACE) mass anomaly time series to be fairly high for
119 the Amazon Basin and Borneo in Southeast Asia. However, other tropical regions showed strong
120 negative correlations with MEI, while arid regions indicated high positive correlations. Phillips
121 et al., (2012) concluded that using GRACE satellite data and ENSO index helped to isolate
122 teleconnection patterns around the globe, showing areas where ENSO and TWS were highly
123 correlated. Other studies that have employed GRACE to study climate-related impacts include
124 Chen et al., (2010), Becker et al., (2010), Thomas et al., (2014), Zhang et al., (2015), Cao et al.,
125 (2015) and Kushe et al., (2016). Given ENSO's dominant impact on global TWS changes,
126 statistical decomposition techniques are developed and applied in Eicker et al. (2016) and
127 Forootan et al. (2018) to separate variations in TWS that are related to ENSO from the rest,
128 which are called 'non-ENSO' modes. Such separation seems to be significant to understand
129 TWS trends without the impact of extreme events such as those associated with ENSO. These
130 studies, however, are global in nature and those that consider various parts of the African
131 continent do not explore the impact of other major climate indices such as Madden-Julian
132 Oscillation (MJO), and Quasi-Biennial Oscillation (QBO) on TWS changes at continental scale.
133 For instance, Forootan et al, (2014a) showed that there is significant influence of NAO and
134 ENSO on annual and inter-annual variability of TWS over West Africa while Ndehedehe et al.,

135 (2017) examined the association of three global climate indices (ENSO, IOD, and Atlantic
136 Multi-decadal Oscillation AMO) with changes in TWS derived from both Modern-Era
137 Retrospective Analysis for Research and Applications (MERRA, 1980–2015) and Gravity
138 Recovery and Climate Experiment (GRACE, 2002–2014). The present contribution aims at
139 filling this gap by not only considering ENSO, IOD, and NAO that have been treated in parts of
140 Africa as discussed above, but also two additional climate indices (i.e., MJO and QBO), which
141 have not previously been considered, and are also known to influence seasonal and intra-seasonal
142 rainfall variability over parts of Africa (e.g. Semazzi and Indeje, 1999). For the first time, a study
143 of the linkages between these five major climate indices and TWS is undertaken over the entire
144 continent of Africa, known to be in-situ data deficient. This pioneering continent-wide study of
145 climate variability impacts on the stored water of the continent will provide useful information
146 for some areas that have hardly been covered. Our hypothesis in this study is that generally all
147 the five global climate indices are linked to sub-seasonal and inter-annual patterns and anomalies
148 of rainfall over Africa (cf. Figure 1). Hence, the same indices, at times individually or in
149 combinations, could most likely have a significant influence on the variability of TWS at
150 seasonal to inter-annual time scales over the continent. Therefore, one can consider the temporal
151 patterns of the climate indices as known, and try to find similar patterns in TWS time series. This
152 has been done here by computing linear correlations that are described in the next section along
153 with a brief description of the different datasets used in this study.

154
155 Therefore, the present study specifically contributes the following; (i) it provides an analysis of
156 possible linear and non-linear relationships between five common global climate indices (NAO,
157 QBO, ENSO, IOD, MJO) and GRACE-derived TWS data (hereafter referred to simply as
158 GRACE-TWS) over the entire African continent, (ii), it provides an analysis of both phase-
159 locked and lagged correlations between these key global climate indices and TWS changes at
160 sub-seasonal, annual, and decadal time scales, and (iii), it applies a higher order statistical
161 method of Independent Component Analysis (ICA, Forootan and Kusche, 2012, 2013) to filter
162 the interrelationships among the five global climate indices and isolate any unique or combined
163 influences of these indices on TWS changes of the African continent. This enables identification
164 of unique regions where such relationships are strongest, which is important for water resources
165 assessments and management.

166
167 The rest of this study is organized as follows; in section 2, the study domain is presented, while
168 section 3 briefly describes the five global climate indices that have been correlated with TWS
169 data in this study. Section 4 analyses and discusses the results Section 5 provides the major
170 conclusions of the study.

171
172
173

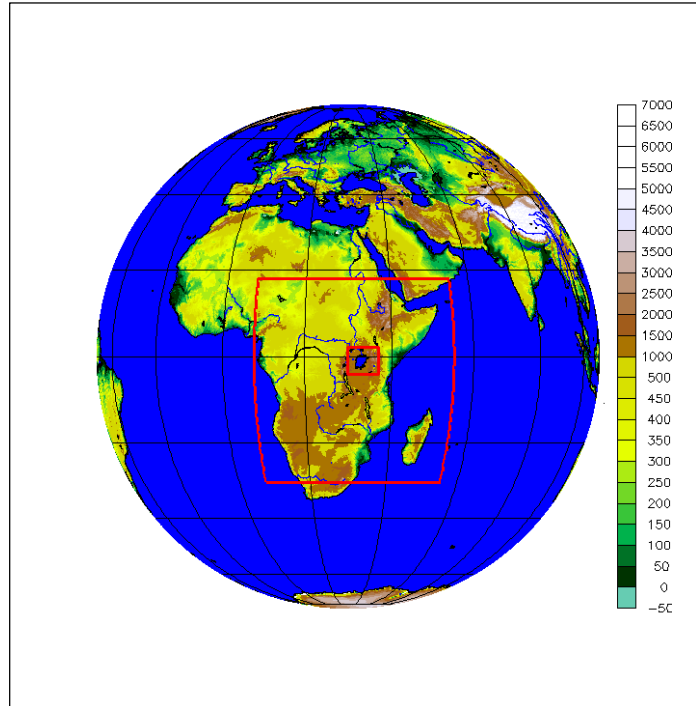


Figure 1 Study domain. Interior boxes feature sub-Saharan Africa (SSA) and Lake Victoria Basin (Largest Freshwater surface in Africa). The colors show elevation in meters.

174
175
176
177

2.0 Data and Methods

178
179

The data used include; monthly time series of GRACE-TWS, NOAA's Multivariate ENSO Indices (MEI), IOD data from Japanese Agency for Marine Earth-Science Research and Technology (JAMSTEC), QBO and NAO indices (from NOAA archive). Detailed descriptions of these data sets are presented in what follows.

183
184

2.1 Gravity Recovery And Climate Experiment (GRACE)

185
186

The GRACE mission, launched in 2002, is a joint US National Aeronautics and Space Administration (NASA) and the German Aerospace Centre (DLR) gravimetric mission aimed at providing spatio-temporal variations of the Earth's gravity field. On time scales ranging from months to decades, temporal variations of gravity are mainly due to redistribution of water mass in the surface fluid envelopes of the Earth. Over land, GRACE provides measurements of vertically integrated terrestrial water storage (TWS) changes, which include surface water, soil moisture, groundwater, snow over large river basins, and biomass (see, e.g., Tapley et al., 2004; Khaki et al., 2017a). Monthly GRACE-TWS data used in this study were obtained from the German Research Centre for Geosciences Potsdam (GFZ). Version (RL05a) of GRACE level-2 data ($1^0 \times 1^0$ spatial resolution) from GFZ that are derived in terms of fully normalized spherical harmonic (SH) coefficients of the geopotential fields up to degree and order 90 were downloaded from the Information System and Data Centre (ISDC) (<http://isdc.gfz-potsdam.de/index.php>) and used to compute monthly TWS fields. First, GRACE Level-2 solutions were augmented by the degree-1 (<https://grace.jpl.nasa.gov/data/get-data/geocenter/>) in order to include the variation of the Earth's center of mass with respect to a crust-fixed reference system. This replacement is

199
200
201

202 undertaken due to its impact on the amplitude of the annual and semi-annual water storage
203 changes. Degree 2 and order 0 (C20) coefficients from GRACE (Cheng et al., 2014; Khaki et al.,
204 2017b, 2017c) are not well determined and were replaced using JPL products
205 (<http://grace.jpl.nasa.gov/data/get-data/oblateness/>).

206
207 GRACE level-2 spherical harmonics at higher degrees are affected by correlated noise (e.g.,
208 Khaki et al., 2018) and are therefore filtered using the DDK3 de-correlation filter (similar to that
209 of Kusche et al., 2009). Selecting DDK3 for filtering GRACE products makes a good sense since
210 GFZ RL05a data represents considerably lower noise than the previous release of the GRACE
211 level-2 data. Monthly DDK3 filtered solutions were then used to generate TWS grids over Africa
212 following the approach of Wahr et al., (1998). Since the signals over land areas are of interest to
213 this study, the ocean areas were masked using a sea-land mask similar to the mask that is used to
214 generate GRACE-AOD1B de-aliasing products (<http://www.gfz-potsdam.de/AOD1B>).

215

216 **2.2 Global Climate Indices**

217 All four indices for ENSO, QBO, MJO, and NAO used in the study are derived from those
218 computed at NOAA, but IOD from the Japanese Marine-Earth Science and Technology
219 (JAMSTEC), and are briefly described in the subsequent sub-sections.

220

221 *2.2.1 Multivariate ENSO Index (MEI)*

222

223 MEI (<http://www.esrl.noaa.gov/psd/enso/mei/>) is the first principal component of the combined,
224 normalized fields of sea level pressure, zonal and meridional components of wind, surface air
225 pressure, and total cloudiness fraction. The units of MEI are standardized and hence a score of 1
226 represents a full standard deviation departure of the principal component for the respective
227 season involved (Wolter and Timlin, 2011). A comparison of MEI and Nino3.4 indices in this
228 study found the negligible difference between the correlation values computed (as will be
229 demonstrated in the results discussed later in this contribution). NOAA's monthly MEI (2003 to
230 2014) is utilized in this study, where they are correlated with TWS time series over the same
231 time period.

232

233 *2.2.2 Indian Ocean Dipole (IOD) Index*

234

235 Indian Ocean Dipole (IOD) is an irregular oscillation of sea-surface temperatures, in which the
236 western Indian Ocean becomes alternately warmer or colder than the eastern part of the ocean. It
237 is represented by anomalous SST gradient between the western equatorial Indian Ocean and the
238 southeastern equatorial Indian Ocean, where this gradient is often referred to as Dipole Mode
239 Index (DMI). In this study, the instantaneous and lagged monthly correlations between DMI
240 (<http://www.jamstec.go.jp/frcgc/research/d1/iod/HTML/Dipole%20Mode%20Index.html>) and
241 TWS data over the period 2003-2014 are analyzed.

242

243 *2.2.3 Quasi-Biennial Oscillation (QBO) Index*

244

245 QBO (<http://www.esrl.noaa.gov/psd/data/correlation/qbo.data>) involves the fluctuation between
246 equatorial westerly and easterly wind regimes in the lower stratosphere with a period of about
247 26-29 months. This oscillation is discerned through an index that is based on a calculation of

248 zonal wind anomaly at 30hPa averaged along the equator (u-30 QBO) or at 50hPa (u-50 QBO).
249 Lau and Shoo (1988) suggested the link between the easterly phase of QBO and ENSO. In the
250 present study, QBO zonal index computed from NCEP/NCAR Reanalysis data at 30hPa level
251 (i.e. u-30 QBO) covering the period 2003-2014 is utilized.

252

253 *2.2.4 Madden-Julian Oscillation (MJO) index*

254

255 The Madden-Julian Oscillation (MJO; Madden and Julian 1971, 1972) is a tropical atmospheric
256 phenomenon first recognized in the early 1970s and is also commonly known as the 40-day
257 wave. This wave often develops over the Indian Ocean and then travels east across the tropics at
258 5-10 m/s. The MJO has been suggested as a key factor in connecting or bridging weather and
259 climate, and thus at times very important in influencing rainfall over eastern Africa, including the
260 Lake Victoria Basin (see, e.g., Omeny et al., 2008). The MJO data used in this study was
261 obtained from Climate Prediction Center (CPC) archive for the period 2003-2014
262 (http://www.cpc.noaa.gov/products/precip/CWlink/daily_mjo_index/mjo_index.html).

263

264 *2.2.5 North Atlantic Oscillation (NAO) Index*

265

266 The NAO (<http://www.cpc.ncep.noaa.gov/products/precip/CWlink/pna/nao.shtml>) consists of a
267 north-south dipole of anomalies, with one center located over Greenland and the other center of
268 opposite sign spanning the central latitudes of the North Atlantic between 35°N and 40°N. Both
269 negative and positive phases of the NAO are associated with basin-wide changes in the intensity
270 and location of the North Atlantic jet stream and storm track and in large-scale modulations of
271 the normal patterns of zonal and meridional heat and moisture transport, which in turn results in
272 changes in global temperature and precipitation patterns. NAO data for the period 2003-2014
273 was employed in this study.

274

275 **3.0 Results and Analysis**

276 The study analyses both instantaneous and lagged relationships between the five global climate
277 teleconnection indices and GRACE-TWS using Pearson correlations, and Independent
278 Component Analysis (ICA) technique. Possible lagged relationships are also explored by
279 removing annual and semi-annual cycles from both climate indices and GRACE-TWS products
280 to isolate potential seasonal dependence of total water storage changes on the dominant seasonal
281 rainfall patterns over most parts of Africa. Further, in order to minimize redundant information
282 between climate indices, due to their overlapping inter-relationships, the ICA technique (see e.g.,
283 Forootan and Kusche, 2012 and 2013) is applied. This is accomplished by performing
284 correlations between the dominant independent patterns of climate indices and GRACE-TWS
285 changes. In order to provide a measure of an average influence of each climate index on TWS
286 changes over the period of our study, the normalized time series of each index along with a linear
287 trend and annual/semi-annual cycles are fitted to the time series of TWS changes in each grid as:

288

$$289 \quad x(i, j, t) = a + bt + c \sin(2\pi t) + d \cos(2\pi t) + e \sin(4\pi t) + f \cos(4\pi t) + g I +$$
$$290 \quad h H(I(t)) + \varepsilon(t) \text{Eq (1),}$$

291

292 where i and j represent the location of the grid, t is time in years, $H(I(t))$ represents a Hibert
293 transformation of the normalized climate index, which is the same as I but after shifting by $\pi/2$

294 in the spectral domain, and $\varepsilon(t)$ represents the temporal residuals. Coefficients a to h are
295 computed using the least squares approach. The influence of the five global climate indices on
296 TWS variability is then examined to identify possible “hot-spots”, where changes in TWS are
297 significantly influenced by a specific or a combination of the indices (i.e., ENSO, IOD, QBO,
298 MJO, and NAO), and whether there exists phase-locked or lagged relationships. In the following
299 sections the influence of g that also indicates the possible contributions of each index (or their
300 combinations) in TWS changes are presented.

301

302 *3.1 Instantaneous Pearson Correlation and Amplitude Analysis.*

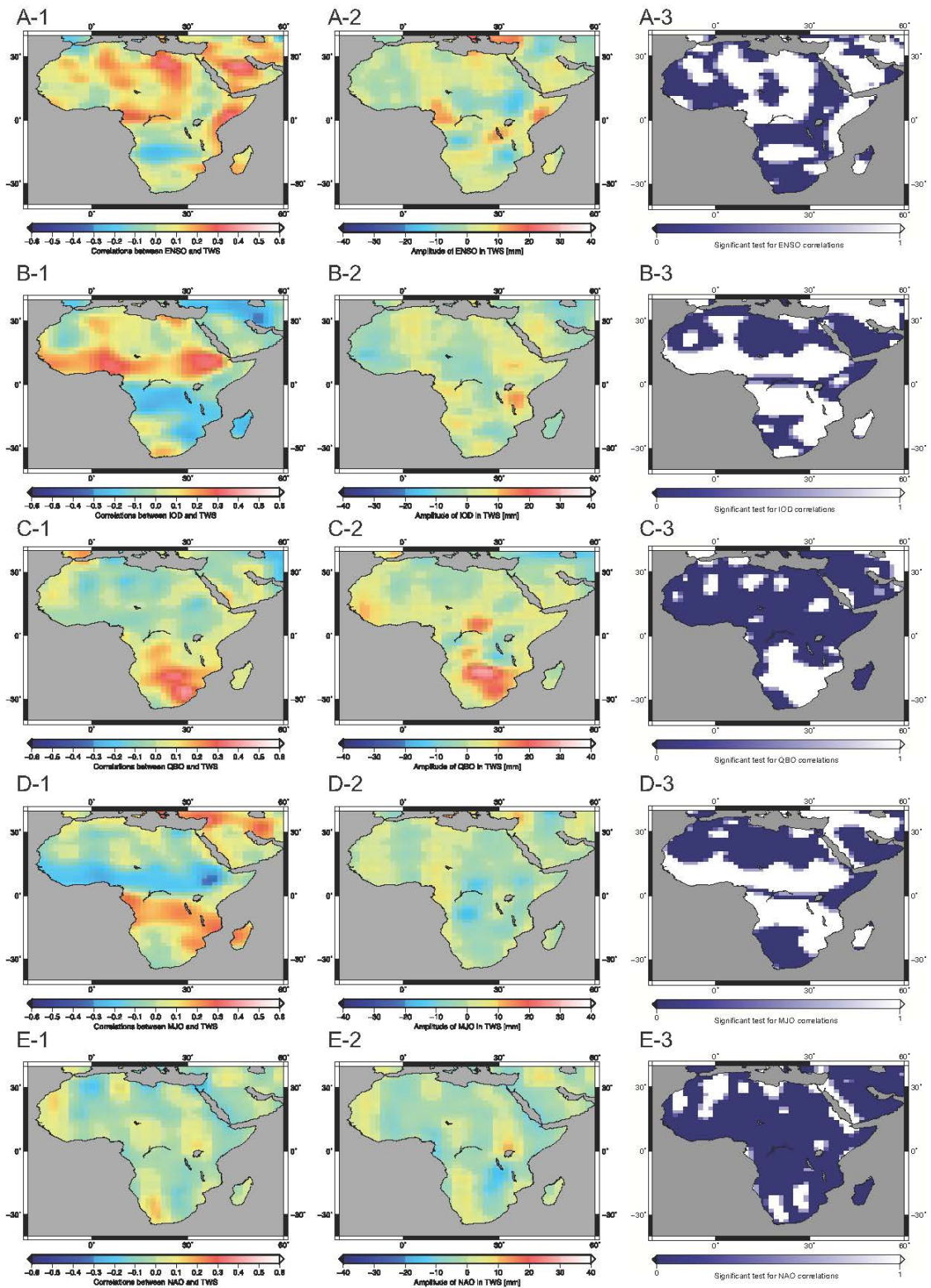
303 Instantaneous correlations (lag-0) between the five climate indices and TWS during the period
304 2003-2014 are presented in Figure 2. Note that the amplitudes of the r-values indicate whether
305 the effect of a particular climate index represents positive or negative change in monthly TWS
306 (e.g., Figure 2 A2-E2). The amplitude of each index (g in Eq. (1)) is shown in millimeters (mm)
307 i.e., the middle panels of Figure 2 (A2-E2). The statistical significance of their-values at 95%
308 confidence level are presented on the right panel (A3-E3), where zero (0) indicates non-
309 significant correlations and 1 is significant. The correlation analysis is undertaken considering
310 different levels of noise in TWS data. Values between 0 and 1 in the right panel indicate regions
311 where the estimated correlations are accepted when the noise level is less than 1 cm, and they are
312 rejected when the noise levels are considerably higher.

313

314 GRACE- TWS and ENSO are highly correlated (positive) primarily along the western coast of
315 the Indian Ocean/East Africa coast (Figure 2: A-1). Also, positive correlations between ENSO
316 and TWS occur along the West African coast, especially coast of Guinea, in the Mediterranean,
317 as well as over central parts of the Sahel. These findings support the work of Ndehedehe et al.,
318 (2017), which found strong presence of ENSO-induced TWS derived from MERRA reanalysis
319 data in the coastal West African countries and most of the regions below latitude 10°N .
320 However, TWS and ENSO are mostly negatively correlated over central Africa (especially over
321 the Congo Basin/Forest) and parts of South Africa, western Ethiopia and most parts of Sudan.
322 The correlations are significant over the coastal regions of the Horn of Africa although the
323 amplitudes (mm) are fairly low (Figure 2: A-1 - A-3). Over the equatorial central/eastern Africa
324 and the coast of Guinea, however, the amplitudes are greater than 10 mm/month implying that
325 ENSO-related precipitation induces an increase of about 10 mm/month or more in TWS (Figure
326 2: A-2).

327

328 Pearson correlations between IOD and TWS reveal a unique dipole correlation pattern with
329 strong positive correlations with amplitudes exceeding 10 mm/month over the southern margins
330 of the Sahel, but large negative correlations (with amplitude less than -10mm/month) are
331 dominant over central and eastern Africa, and particularly over the Congo Basin (Figure 2:B-1
332 and B-2). It is notable that over equatorial eastern Africa, these correlations are somehow
333 opposite to the expected wet/dry anomalies associated with positive/negative IOD phases (e.g.,
334 Saji et al., 1999), which might be due to the short period of the dataset used in the present study.
335 However, several other factors including the complex terrain over East Africa can influence the
336 spatial organization of surface and sub-surface water patterns in return leading to TWS patterns
337 that may be inconsistent with known IOD-rainfall relationships.



338

339
340

Figure 2 correlations between the five climate indices and TWS during the period 2003-2014 (A-1-E-1), the amplitude of each index (A-2-E-2), and the statistical significance of the r -values at 95% confidence level (A-3-E-3).

341 Statistically significant, positive, correlations between QBO and TWS are also found over
342 southern Africa (Figure 2: C-1, C-2, and C-3). However, the impact of MJO on monthly TWS
343 changes over Africa is dominated by a dipole pattern, characterized by large negative r-values
344 over southern margins of the Sahel (Figure 2: D-1 to D-3), extending into western Ethiopia and
345 over the coast of West Africa, and large positive r-values over equatorial central Africa/Congo
346 Basin and southwestern coast of Indian Ocean (i.e., southern parts of East Africa extending into
347 Tanzania and Mozambique). In contrast, the NAO index apparently displays no strong influence
348 on TWS changes over Africa (Figure 2:E-1 to E-3) based on instantaneous correlations with
349 monthly data.

350

351 *3.2 Lagged Pearson Correlations and Amplitude Analysis*

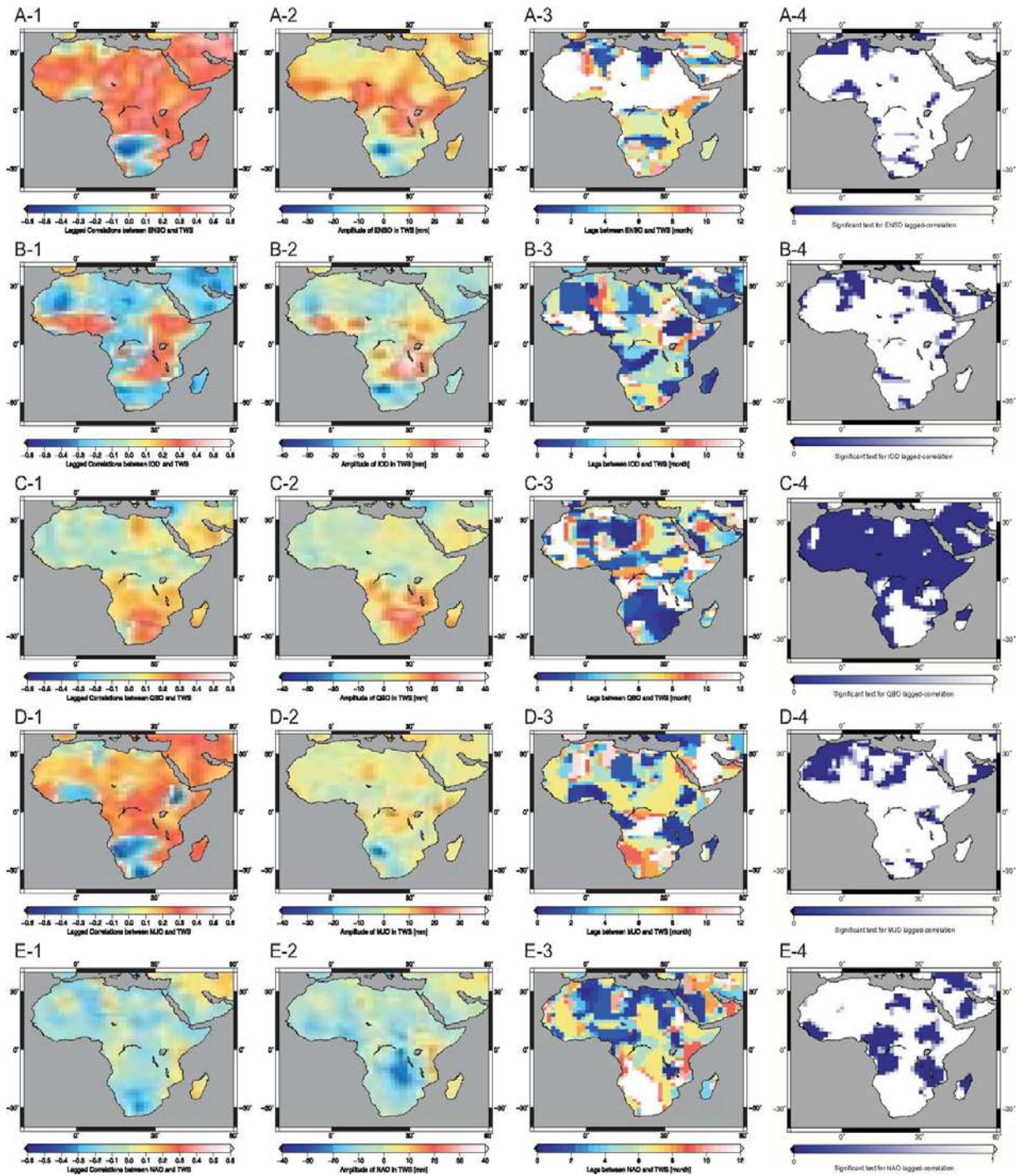
352 To examine if there existed any lagged relationships between TWS changes and the five global
353 climate indices given the fact that for hydrological processes, a temporal lag usually exists
354 between changes in fluxes (precipitation, evapotranspiration, and runoff) and the peak of water
355 storage (see e.g., Awange et al., 2013), lagged Pearson correlation analysis is done (e.g., Figure
356 3). Furthermore, global climate teleconnections such as ENSO often lead to shifts in global
357 climatic patterns such as east-west displacement of the Walker circulation over equatorial eastern
358 and central Africa that might impose lead/lag time of up to 6 months (e.g., Indeje et al., 2000).
359 Hence, ENSO could as well affect the seasonal and inter-annual variability of TWS. In Figure
360 3:A-1, our results show that most regions (north of 15°S) apparently display very strong lagged
361 relationships/correlations between ENSO and TWS that include an 8-12 and 4-8 month lagged
362 relationships over the Sahel and equatorial eastern Africa, respectively (Figure 3:A-3). However,
363 significant negative correlations between ENSO and TWS over southern Africa appear to be
364 more phase-locked (lag=0). But, unique lagged relationships between TWS and IOD are found
365 particularly over equatorial eastern (around Lake Victoria Basin) and central Africa, where the
366 amplitudes of the influence are found to be greater than 20 mm/month especially within 2-6
367 month lags (Figure 3: B-2, B-3, B-4).

368

369 The lagged correlations computed between QBO index and TWS display fairly strong positive
370 relationship over southern Africa (Figure 3: C-1) especially with 2-month lag (Figure 3: C-3).
371 However, very low (insignificant) QBO-TWS correlations exist over the rest of sub-Saharan
372 Africa as shown in Figure 3: C-4. One of the possible reasons is that QBO time scale is in the
373 intervening period between that of ENSO (3-5 yrs) and IOD (2-5 yrs) and hence the QBO is
374 highly likely masked by the stronger ENSO and IOD signal given also that our study period
375 covered only 10 years.

376

377 In Figure 3: D, the relationships between MJO and TWS are explored. It should be noted that
378 even though the periodicity of MJO is approximately 30-90 days, we believe that the monthly
379 time series of TWS and MJO index covering the 13-year period of our study is long enough to
380 capture the right phases of MJO and possible relationships with TWS changes. As a whole, the
381 MJO index is found to be positively/negatively correlated with TWS over northern sub-Saharan
382 Africa/southern Africa (Figure 3: D-1), with MJO-TWS relationship over southern Africa
383 appearing to be strong within 6-8 months lag (Figure 3: D-1, D-3). The amplitudes of the
384 influence are however considerably smaller than other induces (compare Figure 3: D2 with other
385 plots on the same column).



387

388 *Figure 3 lagged correlations between the five climate indices and TWS (A-1-E-1), the amplitude of each index (A-2-E-2), 2-month*
 389 *time lag between the indices and TWS (A-3-E-3), and the statistical significance test for lagged-correlation (A-4-E-4).*

390

391 With regard to the potential relationships between NAO and TWS variability over sub-Saharan
 392 Africa, our analysis reveals that the only regions where significant lagged correlations exist are

393 over the western part of southern Africa. The r-values over these regions are also significant at
394 95% confidence level, especially at 8-12 month lag (Figure 3: E-3 and E-4).

395

396 To ensure that the results described above are robust enough, we perform further analysis of the
397 correlations between TWS and climate indices after filtering out seasonal cycle (semi-annual and
398 annual cycles) from the monthly time series of the five indices. Part of the reason for doing this
399 is due to the dominant role of ITCZ that drives the seasonality of climate, especially rainfall over
400 Africa. The results are discussed in detail in the next section.

401

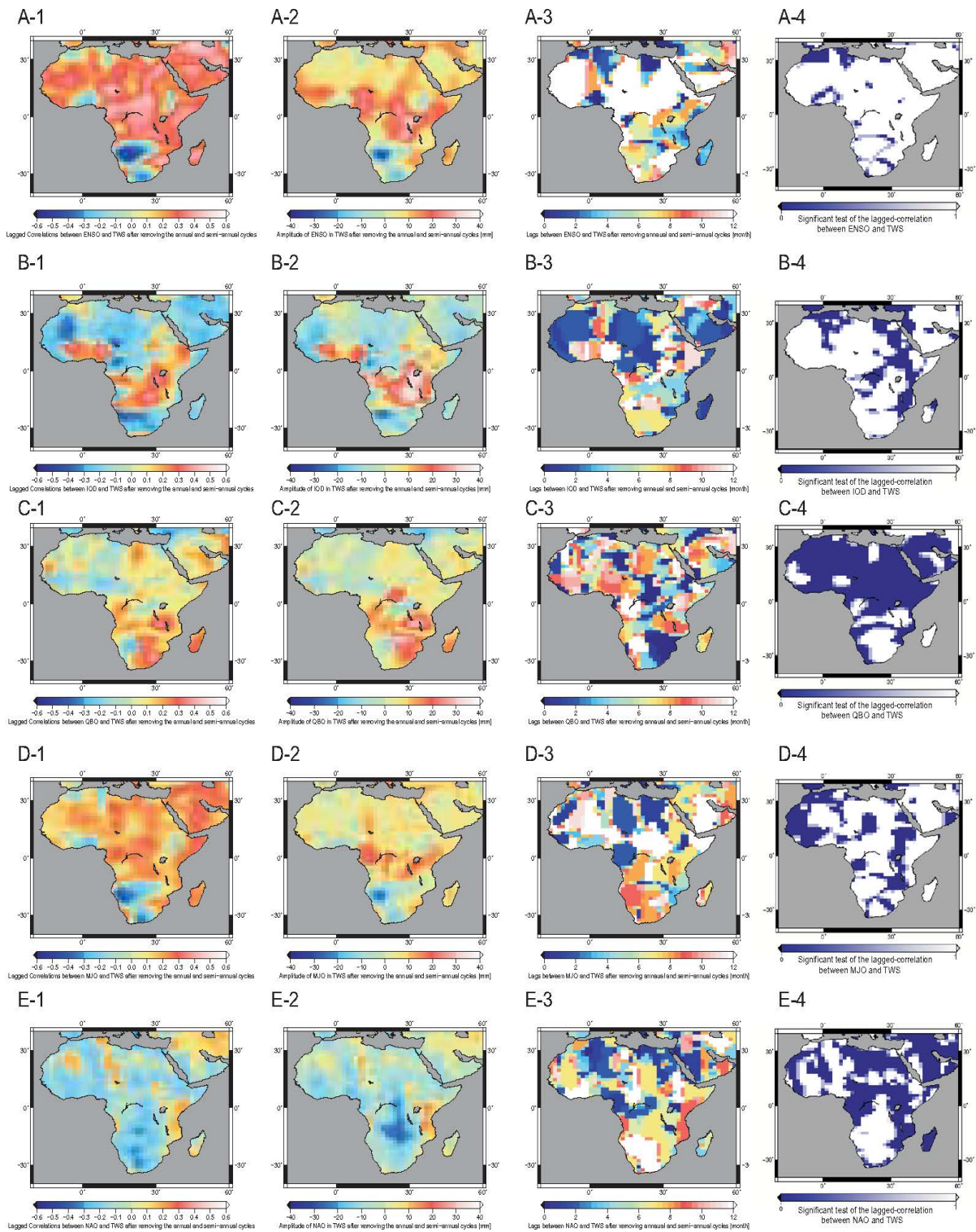
402 *3.3 Lagged Correlation and Amplitudes after Filtering Annual and Semi-annual Cycles*

403 The north-south migration of ITCZ and external forcing associated with global atmospheric
404 circulation and sea surface temperature (SST) perturbations (e.g. Giannini et al., 2003) has been
405 shown to be partly responsible for the strong seasonal variability of precipitation over Africa. We
406 investigate if the variability of TWS is also in synch with the seasonal and inter-annual
407 variability of precipitation, in response to five global teleconnection indices. Generally, the
408 correlations between the five indices (ENSO, IOD, NAO, MJO, QBO) and TWS are relatively
409 stronger, with annual/semi-annual cycles filtered from the time series, suggesting apparent
410 climate-TWS association at inter-annual scale (see Figure 4). For instance, in Figure 4: A-1 to A-
411 4, the correlation between ENSO and TWS is found to be more significant over many parts of
412 Africa when the seasonal cycle is filtered from the ENSO index, compared to cases where
413 seasonal cycle is unfiltered(cf. Figure 3: A-1) although the spatial patterns remains the same.
414 This implies that strong ENSO-TWS relationship is more pronounced when semi-annual and
415 annual cycles are filtered. However, statistically significant ENSO-TWS r-values greater than 0.4
416 (using 137-month time series: 2003-2013) tended to occur with 6 to 12 months lags, especially
417 over the Sahel and the Horn of Africa (Figure 4: A-3 and A-4).

418

419 Similarly, the IOD-TWS relationships after annual/semi-annual cycles are filtered also depict
420 very strong lagged correlation (more than 0.4 with lags of 2 to 6 months), particularly over
421 equatorial central Africa and Lake Victoria Basin in eastern Africa (Figure 4: B-1 to B-4).
422 However, areas depicting strong QBO influence on TWS at inter-annual and longer time scales
423 tend to be confined mostly over southern Africa (Figure 4:C-1 to C-4). MJO-TWS relationship is
424 presented in Figure 4: D-1 to D-4, which shows strong relationship over southern Africa within
425 6-8 months lags (see also Figure 2: D). Finally, the potential NAO-TWS relationships through
426 lagged correlation after filtering the seasonal cycle from the time series tend to be dominated by
427 very large negative correlations over southern Africa (Figure 4: E-4), but virtually uncorrelated
428 over the rest of the continent.

429



430

431 *Figure 4 Lagged Correlations between the five indices and TWS (A-1-E-1), the amplitude of each index A-2-E-2), lags between the*
 432 *indices and TWS A-3-E-3), and the statistical significance test for lagged-correlation (A-4-E-4). Note that annual and*
 433 *semi-annual cycles are removed before these processes.*

434 Overall, both lagged and instantaneous correlations between individual climate indices (CI) and
 435 TWS produce unique regions, where the CI-TWS connections/relationships are very strong (see
 436 Table 1 for a summary). This is the same for cases both with and without the semi-annual and
 437 annual cycles filtered from the time series of the climate indices during the 137-months' period,
 438 spanning 2003-2013. In addition, it is worth noting that for some indices (e.g., ENSO and IOD),
 439 the interpretation of possible physical processes/drivers linked to their TWS relationships must
 440 be done with caution. This is due to the fact that ENSO and IOD are sometimes highly
 441 interrelated, posing challenges in separating their unique and/or combined influences on regional
 442 or continental precipitation and TWS patterns. In other words, isolating their unique/combined
 443 contributions (correlation) to TWS variability at monthly, seasonal, inter-annual and longer time
 444 scales is challenging. Hence, in the next section, the statistical interdependence between/among
 445 climate indices are accounted for using Independent Component Analysis (ICA, Forootan and
 446 Kusche, 2012, 2013).

447
 448 Table 1: Summary of the influence of global indices on TWS

Index/Mode	Impact on TWS	Regions with the strong CI-TWS relationship	Remark
ENSO	Negatively correlated Positively correlated	Southern Africa Eastern Africa Sahel	No lag No lag 6-12 month's lag
IOD	Positively correlated	Eastern Africa Central Africa (Congo Basin)	2-6 month's lag
QBO	Positively correlated	Southern Africa	2 month's lag
MJO	Positively correlated	Congo Basin Southern Africa	No lag 4-6 month's lag
NAO	Positively correlated	Southern Africa	6-8 month's lag

449
 450

451 *3.4 ICA-derived Isolation of Redundant Information Between Climate Indices*

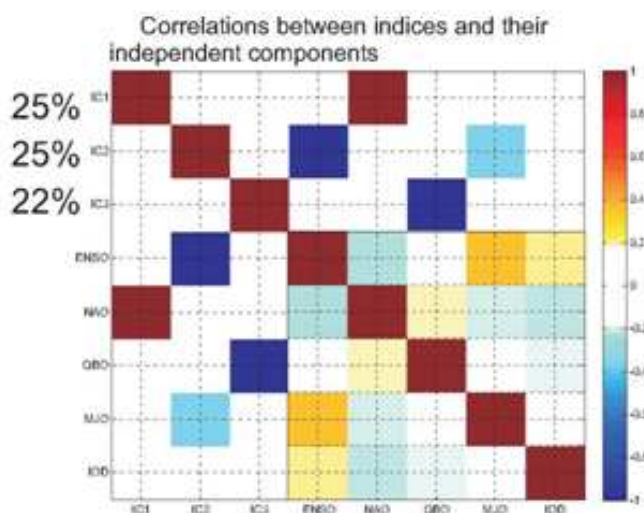
452 ICA is applied to the time series of climate indices in order to explore the existence of any
 453 significant modes of monthly and inter-annual variability of TWS over Africa that may be linked
 454 to specific or combined global climate indices (see Table 2). The time series of the three leading
 455 Independent Components (ICs) are retained and correlated with respective time series of the five
 456 climate indices. From a statistical point of view, ICA technique makes use of the higher order
 457 (higher than second order mutual statistical information) between climate indices to extract
 458 modes that are statistically mutually as independent as possible (see Forootan, 2014 for more
 459 details). Applying ICA is equivalent to defining a linear relationship (shown by a mixing matrix
 460 **A**) between observations (available CIs stored in matrix **X**) and temporally independent
 461 components ICs (stored in matrix **S**)

$$\mathbf{X} = \mathbf{AS}.$$

462 Here **A** is computed by making the fourth-order cumulant's tensor based on the time series of
 463 CIs as diagonal as possible as outlined in Forootan and Kusche (2012).

464
 465 In Figure 5, the correlation matrix of the estimated Independent Components (ICs) from the
 466 climate indices (CIs) versus individual climate indices is presented, and generally, the ICA
 467 technique is able to isolate the redundant information between CIs well. The first ICA mode
 468 (IC1) is seen to be highly correlated with NAO (positive), while the second ICA mode (IC2) is
 469 highly correlated to ENSO (negative) and modestly correlated to MJO (negative). IC3 is highly
 470 correlated with QBO (negative). Therefore, no duplicated correlations are seen between ICs and
 471 the indices (i.e., no climate index is correlated with more than one IC, see Figure 5). This means
 472 that the leading modes of ICA have the potential to distinguish between the unique or combined
 473 contributions/relationships of the global climate indices and TWS changes. We also note that
 474 none of the ICs are correlated with IOD. Tables 3 show the actual correlation while Figure 5
 475 provides a visual clarity.

476



477

478 *Figure 5 Correlation between the indices and their Independent Components*

479

480 Table2: A summary of the influence of the leading Independent Components (ICs) on TWS

ICA Mode	Impact on TWS	Regions with strong IC-TWS relationship/correlation	Remark
IC1	Reduction in TWS	Eastern Africa Southern Africa	Greater than 10mm/month reduction Occurs 6-8 month's lag
IC2	Reduction in TWS	Sahel, Central Africa	-
IC3	Unclear influence	All sub-Saharan Africa	-

481

Table 3: Correlations (at 95% confidence level) between leading Independent Components and global climate indices

IC1	1							
IC2	0.01	1						
IC3	-0.1	0.0	1					
ENSO	0.01	-0.8	0.0	1				
NAO	0.9	0.0	0.0	-0.3	1			
QBO	0.1	0.0	-0.8	0.0	0.2	1		
MJO	0.1	-0.3	-0.1	0.4	-0.2	0.0	1	
IOD	0.01	0.01	0.0	0.2	-0.3	-0.2	0.0	1
	IC1	IC2	IC3	ENSO	NAO	QBO	MJO	IOD

483

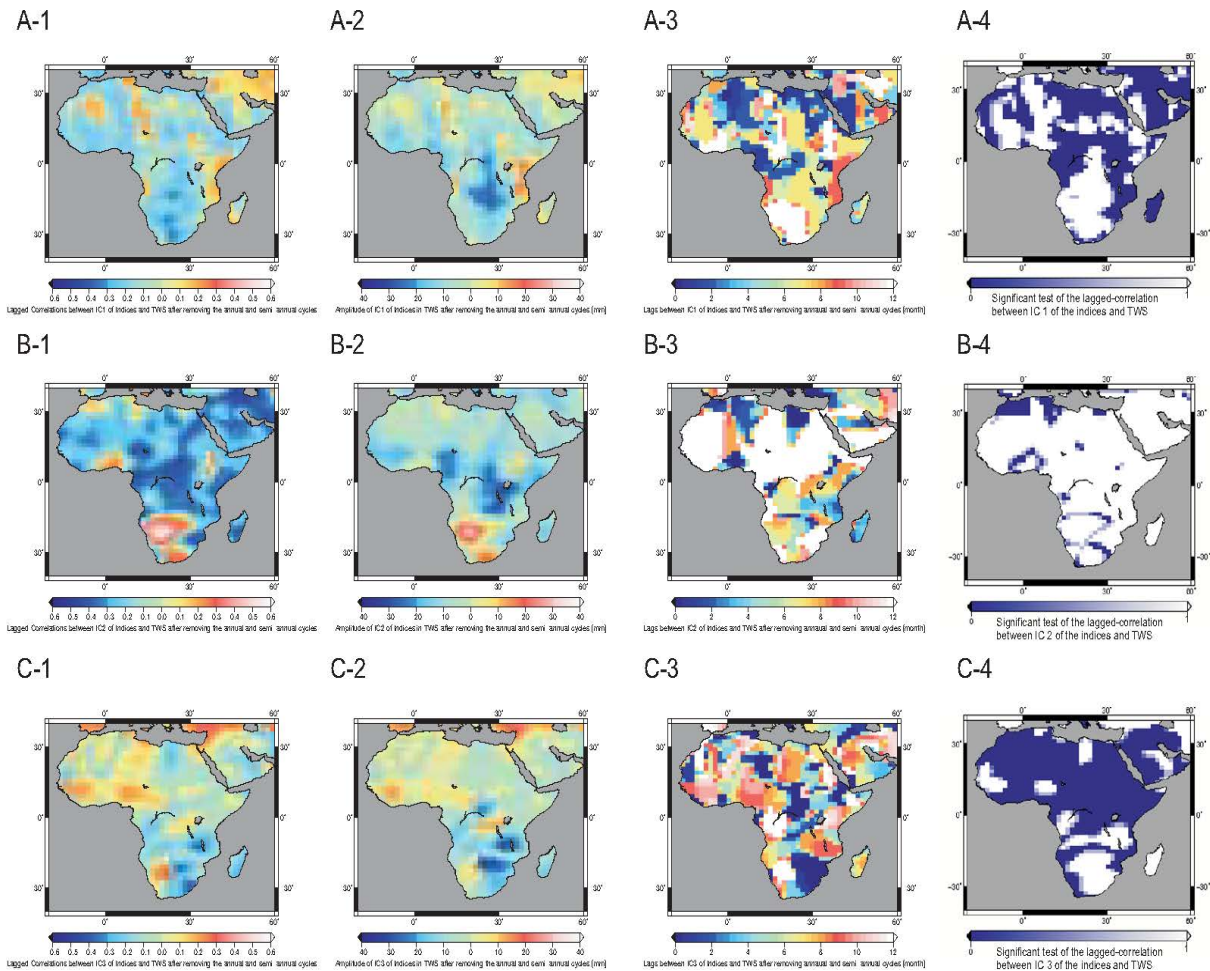
484 3.5 Correlations between Leading ICA Modes of Climate Indices and GRACE-TWS

485 The lagged correlations between IC1 and TWS, after removing the seasonal cycles, are shown in
 486 Figure 6: A-1. The large negative r-values over southern and equatorial Africa (especially over
 487 the Congo Basin), also co-located with regions of reduced TWS of 10mm/month or less are very
 488 conspicuous. The r-values also tended to be larger (negative; <-0.4) and significant at 6-12
 489 months lags. This likely implies that the influence of NAO on TWS (see, Figure 5-B) is very
 490 strong over parts of southern Africa and the Congo Basin (Figure 6: A-3 and A-4) several
 491 months after the peak NAO events. The lagged correlations between IC2 and TWS, after filtering
 492 semi-annual cycle from TWS time series (Figure 6: B-1) most likely represent a combined
 493 ENSO and MJO influence on TWS changes over parts of Africa.

494

495 Generally, large negative correlations are found over equatorial central Africa/Congo Basin and
 496 most parts of the Sahel. The higher (negative) IC amplitudes (mm) are also co-located with
 497 regions of higher r-values (Figure 6:B-2). The r-values are statistically significant over the Sahel,
 498 especially at 6-8 months lag. This apparently implies that ENSO-related hydroclimate anomalies
 499 tend to reduce TWS over these areas (especially over the Sahel) long after the peak of the ENSO
 500 episodes (Figure 6: B-3 and B-4). This ENSO-TWS relationship does not seem to mimic the
 501 often-witnessed ENSO-rainfall wet/dry dipole pattern over eastern/southern Africa (e.g., Indeje
 502 et al., 2000). This probably implies two points: first there are completely unique regions with
 503 very strong ENSO-TWS relationships, and secondly the time lags for ENSO influence on TWS
 504 are completely different from those of ENSO-rainfall relationship. Finally, in Figure 6: C-1, the
 505 lagged correlations between IC3 and TWS are shown. It should be noted that as shown earlier
 506 (Figure 5) IC3-TWS correlations represents an apparent influence of IOD on TWS. However,
 507 comparing r-values and the amplitudes of IC3 (Figure 6: C-2) and the t-statistics map (Figure
 508 6:C-4), the potential influence of IOD on TWS variability clearly emerges only over southern

509 Africa. A summary of the correlation results between climate indices/their independent
 510 components and TWS changes of Africa over 2003-2014 are summarized in Table 1.
 511



512
 513 *Figure 6 Lagged Correlations between the five indices Independent Components (ICs) and TWS (A-1-E-1), the amplitude of each*
 514 *index's IC (A-2-E-2), lags between the ICs of indices and TWS (A-3-E-3), and the statistical significance test for lagged-correlation*
 515 *(A-4-E-4). Note that annual and semi-annual cycles are removed before these processes.*

516 **4.0 Discussions**

517 The relationships between a mix of global climate indices and total water storage changes have
 518 not been widely investigated, especially over Africa. This study advances understanding of the
 519 inter-relationships between TWS and global climate teleconnection indices in three ways. First,
 520 the correlation and ICA analyses identify possible linear and non-linear relationships between
 521 five primary global climate indices (NAO, QBO, ENSO, IOD, MJO) and GRACE-TWS over the
 522 entire African continent. Secondly, both phase-locked and lagged correlations between these
 523 climate indices and TWS changes at sub-seasonal, annual, and decadal time scales are identified.
 524 Thirdly, through application of higher order statistical method of Independent Component
 525 Analysis (ICA), as in Forootan and Kusche (2012, 2013), the interrelationships among the five
 526 global climate indices are filtered.
 527

528 *4.1 Understanding lagged relationships between global climate indices and TWS*

529

530 Findings from earlier studies involving investigation of linkages between individual climate
531 index/indices and rainfall of different parts of Africa (e.g., Black et al., 2003, Indeje et al., 2000,
532 Mutai and Ward 2001, Indeje and Semazzi, 2000), or with total water storage (TWS) changes
533 (e.g., Awange et al., 2013, Awange et al., 2014, Ndehedehe et al., 2017a, 2018) are broadly
534 consistent with the findings of our study. These studies generally agree in terms of regions where
535 TWS and rainfall variability and patterns tend to follow the dominant seasonality of rainfall over
536 different parts of Africa. However, they provide incomplete understanding of the lagged-
537 relationships between TWS and the primary global climate teleconnection indices, at the
538 continental scale.

539

540 Hassan and Jin (2016) have demonstrated annual phase-lagged relationships between GRACE
541 TWS and rainfall over the major river catchments over Africa, but fall short of clearly attributing
542 causes of the lagged relationships. However, this study finds relatively stronger correlations
543 between the specific and combinations of climate indices and TWS when annual/semi-annual
544 cycles are filtered from the time series. This is apparent in the positive correlations between
545 ENSO and TWS at inter-annual scale, and more pronounced at 6-12 month time lags over
546 equatorial East Africa and the Congo Basin. For other regions the lagged-relationships are
547 summarized in Table 1.

548

549 *4.2 Inter-dependencies between CIs and combined influence on TWS*

550

551 The application of Independent Component Analysis in this study helps to filter redundancies
552 and inter-dependencies between difference CIs thereby ensuring that each ICA mode is attributed
553 to unique influence of TWS by one or a combination of CIs. The inter-relationships between the
554 indices and influence on TWS are summarized in Table 2. Specifically, through ICA analysis,
555 our study is able to demonstrate that the first ICA mode (IC1) is uniquely positively correlated
556 with NAO mostly over southern Africa - meaning significant influence of NAO on TWS changes
557 there, but less likely elsewhere. The inter-relationships between ENSO, IOD, MJO and QBO in
558 influencing inter-annual rainfall variability, as demonstrated in studies of Black et al., 2003,
559 Semazzi and Indeje 2000, and Omeny et al., 2008) are apparent in the second ICA mode (IC2)
560 that is negatively correlated with ENSO and MJO indicating possible combined influences of
561 both indices on TWS-especially over equatorial and central Africa, and over the Niger river
562 basin. Hence, it is possible to isolate unique or combined influences of these indices on TWS,
563 thus pinpoint regions where synchronous or lagged-relationships are strongest, which is
564 important for forward planning, assessments and management of water resources, as well as
565 responding to extreme droughts and floods-often enhanced by global climate
566 teleconnections/indices.

567

568 **5.0 Conclusions**

569 The study investigated the potential influence of five key global climate teleconnection indices
570 on total water storage (TWS) over Africa. Based on Pearson correlation and independent
571 component analysis (ICA) analyses, the study:

- 572 1. Revealed *unique relationships* between TWS and specific global climate indices. In
573 certain cases the regions with the strong climate indices (CI)-TWS connection, e.g.
574 where the indices had significant influences on TWS changes corresponded to areas
575 where previous studies have demonstrated the strong influence of the indices on rainfall
576 anomalies. For, instance, ENSO tended to have a phase-locked positive relationship with
577 TWS over equatorial eastern Africa, consistent with the ENSO-rainfall relationship over
578 the region.
- 579 2. Revealed *unique regions* where CI-TWS relationships were very strong and thus where
580 specific/combination of climate index/indices tended to have a very significant influence
581 on the spatio-temporal variability and changes of TWS. For, example, the apparent
582 ENSO-related influence tended to reduce TWS over certain areas especially over the
583 Sahel with nearly a 6-8 months' time lag. Also, an apparent combined ENSO/MJO
584 negative impact on TWS over equatorial central Africa/Congo Basin and most parts of
585 the Sahel was consistently identified. In addition, NAO seemed to have a significant 6-
586 10 months lagged impact (increase) on TWS over parts of southern Africa and the
587 Congo Basin.
- 588 3. The Pearson correlations and the independent components of climate indices are found to
589 be able to somehow isolate possible contributions (correlations) of single or combined
590 climate indices to TWS changes.
- 591 4. NAO was highly correlated with the leading ICA mode (IC1) over parts of southern
592 Africa and southern Congo Basin. On the one hand, this implied that NAO tended to
593 influence TWS variability over these regions, especially with a time lag of 6-8 months.
594 On the other hand, the lagged correlations patterns between the second ICA mode (IC2)
595 and TWS apparently indicated strong relationships between combined ENSO/MJO
596 indices and TWS changes, with large negative correlations located over equatorial central
597 Africa/Congo Basin and most parts of the Sahel, mostly at 8-12 months' time lag.
- 598 5. Finally, strong lagged correlations between the third ICA mode (IC3) and TWS were
599 stronger over southern Africa and apparently linked to influence of QBO on TWS over
600 the region.

601 Whereas it is obvious that a complex mix of processes may dictate the associations between the
602 global climate teleconnections and continental terrestrial water storage changes, the present study
603 focused mainly on the potential relationships and influence of specific/combined climate indices
604 on TWS changes. As such, it should be noted that some of the confounding factors, not fully
605 considered in our analyses, include e.g., the role of complex terrain especially over the equatorial
606 and the Horn of Africa that potentially can influence surface and sub-surface hydrological
607 processes including changes in the groundwater storage, which in return influences the space-
608 time variability of TWS. Other human-induced activities such as land use patterns and
609 surface/groundwater usage/abstraction might also influence TWS changes but are not necessarily
610 related to possible influences of global climate indices or teleconnections. Finally, it should also
611 be noted that isolating the physical mechanisms through which specific/combined global climate
612 indices might influence TWS changes was beyond the scope of the present study. Instead, the
613 study focused on isolating the possible influence of global climate indices and/or teleconnections
614 on TWS over Africa based primarily on first order statistical correlations and ICA
615 decompositions.

616

617 **Acknowledgments**

618 R. Anyah was supported by US National Science Foundation through Grant #: AGS-1305043. J.
619 Awange appreciates the financial support of Alexander Von Humboldt foundation that supported
620 his stay at Karlsruhe Institute of Technology (KIT), Karlsruhe, Germany, Japan Society of
621 Promotion of Science (JSPS) that supported his stay at Kyoto University Japan and Brazilian
622 Science without Borders Program/CAPES Grant 88881.068057/2014-01, which supported his
623 stay at the UFPE, Brazil. E. Forootan is grateful for the financial supports by the German
624 Aerospace Center (DLR) under the project (D-SAT project - Fkz.: 50 LZ 1402), and the
625 WASM/TIGeR research fellowship from Curtin University. M. Khaki is grateful for the research
626 grant of Curtin International Postgraduate Research Scholarships (CIPRS)/ORD Scholarship
627 provided by Curtin University. The authors are grateful to the GFZ and NASA, and NOAA for
628 providing the GRACE satellite and Global Climate Indices data for this study.

629
630 **6.0 References**

- 631 AghaKouchak, A. (2015), A multivariate approach for persistence-based drought prediction:
632 Application to the 2010-2011 East African Drought, *Journal of Hydrology*, 526, 127-135.
- 633 Agola N. O and Awange J. L. (2014) *Globalized Poverty and Environment 21st Century*
634 *challenges and Innovative Solutions*. Springer, Berlin, New York.
- 635 Agutu, N.O., J.L. Awange, A. Zerihun, C.E. Ndehedehe, M. Kuhn, Y. Fukuda, (2017), Assessing
636 multi-satellite remote sensing, reanalysis, and land surface models' products in
637 characterizing agricultural drought in East Africa, *Remote Sensing of Environment*,
638 Volume 194, Pages 287-302, ISSN 0034-4257, <https://doi.org/10.1016/j.rse.2017.03.041>.
- 639 Anderson, W. B., B. F. Zaitchik, C. R. hain, M. C. Anderson, M. T. Yilmaz, J. Mecikalski,
640 Schultz, L. (2012), Towards an integrated soil moisture drought monitor for East Africa,
641 *Hydrology and Earth System Sciences*, 16, 2893-2913.
- 642 Anyah, R. O. and Semazzi F. H. M. (2004), Simulation of the sensitivity of Lake Victoria basin
643 climate to lake surface temperatures. *Theoretical and Applied Climatology*, 79, 55-69.
- 644 Anyah, R.O., Semazzi F. H. M., L. Xie (2006), Simulated physical mechanisms associated with
645 climate variability over Lake Victoria Basin in East Africa. *Mon. Wea. Rev.*, 134, 3588–
646 3609
- 647 Anyah R.O., and Semazzi F.H.M (2007), Variability of East African rainfall based on multi-year
648 RegCM3 model simulations. *Int. J. Climatol.*: 27, 357-371
- 649 Anyah, R.O., F.H.M. Semazzi, 2009: Idealized simulation of hydrodynamic characteristics of
650 Lake Victoria that potentially modulate regional climate. *International Journal of*
651 *Climatology* 29:7, 971-981
- 652 Awange J.L. and Ong'ang'a, O. (2006), *Lake Victoria: Ecology Resource and Environment*.
653 Springer-Verlag, Berlin, Heidelberg, New York, 354p.
- 654 Awange J. L., Aluoch J., Ogallo L., Omulo M., and Omondi P. (2007), An assessment of
655 frequency and severity of drought in the Lake Victoria region (Kenya) and its impact on
656 food security. *Climate Research* 33 135-142.
- 657 Awange J L, Sharifi M A, Ogonda G, Wickert J, Grafarend E W and Omulo M A (2008), The
658 falling Lake Victoria water level: GRACE TRIMM and CHAMP satellite analysis of the
659 lake basin *Water Resour. Manage.* 22 775–96
- 660 Awange J.L, Anyah, R.O., Agola, N.O, Forootan, E., and Omondi, P.O. (2013), Potential
661 impacts of climate and environmental change on the stored water of Lake Victoria Basin

662 and economic implications. *Water Resources Research*: 49, 8160–8173,
663 doi:10.1002/2013WR014350.

664 Awange J.L, Forootan, E., Kuhn M., Kusche J., Heck B (2014) Water storage changes and
665 climate variability within the Nile Basin between 2002 and 2011. *Advances in Water*
666 *Resources* 73 (2014) 1–15. <http://dx.doi.org/10.1016/j.advwatres.2014.06.010>.

667 Awange, J.L., Khandu, M. Schumacher, E. Forootan, B. Heck, (2016a), Exploring hydro-
668 meteorological drought patterns over the Greater Horn of Africa (1979–2014) using
669 remote sensing and reanalysis products, *Advances in Water Resources*, Volume 94, 2016,
670 Pages 45-59, ISSN 0309-1708, <https://doi.org/10.1016/j.advwatres.2016.04.005>.

671 Awange, J. L., F.Mpelasoka, R. M. Goncalves, (2016b), When every drop counts: Analysis of
672 Droughts in Brazil for the 1901-2013 period, *Science of The Total Environment*,
673 Volumes 566–567, 2016, Pages 1472-1488, ISSN 0048-9697,
674 <https://doi.org/10.1016/j.scitotenv.2016.06.031>.

675 Becker M, Llovel W, Cazenave A, Guntner A, Cretaux JF, (2010), Recent hydrological
676 behavior of the East African great lakes region inferred from GRACE, satellite altimetry
677 and rainfall observations, *Compt. Rend. Geosci.*,342(3), 223-233

678 Black E., J. Slingo, and Sperber K.R., (2003), An observational study of the relationship between
679 excessively strong short rains in coastal East Africa and Indian Ocean SST. *Mon. Wea.*
680 *Rev.*, 31, 74-94.

681 Cao, Y.; Nan, Z.; Cheng, G. (2015), GRACE gravity satellite observations of terrestrial water
682 storage changes for drought characterization in the arid land of Northwestern China.
683 *Remote Sens.*, 7, 1021–1047.

684 Clark, C. O., P. J. Webster, and J. E. Cole (2003), Interdecadal variability of the relationship
685 between the Indian Ocean Zonal Mode and East African Coastal Rainfall Anomalies,
686 *Journal of Climate*, 16, 548-554.

687 Creutzfeldt B., Guntner A., Vorogushyn S., Merz B. (2010), The benefits of gravimeter
688 observations for modelling water storage changes at the field scale. *Hydrol. Earth Sys.*
689 *Sci.* 14(9):1715-1730

690 Eicker, A., Forootan, E., Springer, A., Longuevergne, L., Kusche, J. (2016). Does GRACE see
691 the terrestrial water cycle 'intensifying'? *Journal of Geophysical Research-Atmosphere*,
692 121, 733-745, doi:10.1002/2015JD023808

693 Forootan, E., Kusche, J., Talpe, M.J., Shum, C.K., Schmidt, M. (2018). Developing a complex
694 independent component analysis (CICA) technique to extract non-stationary patterns
695 from geophysical time series. *Surveys in Geophysics*, doi:10.1007/s10712-017-9451-1

696 Forootan, E. (2014), *Statistical Signal Decomposition Techniques for analyzing time-variable*
697 *satellite gravimetry data*, Ph.D. thesis, University of Bonn, Bonn, Germany.

698 Forootan E., Kusche J., Loth I., Schuh W-D., Eicker A., Awange J., Longuevergne L.,
699 Diekkrueger B., Schmidt M., Shum C.K., (2014a). Multivariate prediction of total water
700 storage anomalies over West Africa from multi-satellite data. *Surveys in Geophysics*, 35,
701 Pages 913-940, doi:10.1007/s10712-014-9292-0.

702 Forootan, E., and Kusche, J. (2013), Separation of deterministic signals, using independent
703 component analysis (ICA). *Stud. Geophys. Geod.* 57, 17-26, doi:10.1007/s11200-012-
704 0718-1.

705 Forootan, E., and Kusche, J. (2012). Separation of global time-variable gravity signals into
706 maximally independent components. *Journal of Geodesy*, 86 (7), 477-497,
707 doi:10.1007/s00190-011-0532-5.

708 Goddard, L., and N.E. Graham, (1999), Importance of the Indian Ocean for simulating rainfall
709 anomalies over eastern and southern Africa. *J. Geophys. Res.*, 104, 19,099-19,116.

710 Hassan, A., and Jin, S., 2016: Water storage changes and balances in Africa observed by
711 GRACE and hydrologic models. *Geodesy and Geodynamics*, 7(1), 39-49

712 Indeje M, Semazzi, F.H.M., Ogallo,L.J., 2000: ENSO signals in East African rainfall seasons.
713 *Int. J. Climatol* 20: 19–46

714 Indeje, M., and Semazz, F.H.M., (2000), Relationships between QBO in the lower equatorial
715 stratospheric zonal winds and east African seasonal rainfall. *Meteor. Atm.* 73(3-4), 227-
716 244.

717 Khaki, M., Schumacher, M., J., Forootan, Kuhn, M., Awange, E., van Dijk, A.I.J.M., (2017a)
718 Accounting for Spatial Correlation Errors in the Assimilation of GRACE into
719 Hydrological Models through localization. *Advances in Water Resources*, 108:99-112,
720 doi:10.1016/j.advwatres.2017.07.024.

721 Khaki, M., Hoteit, I., Kuhn, M., Awange, J., Forootan, E., van Dijk, A.I.J.M., Schumacher, M.,
722 Pattiaratchi, C., (2017b). Assessing sequential data assimilation techniques for integrating
723 GRACE data into a hydrological model. *Advances in Water Resources*, 107:301-316,
724 doi:10.1016/j.advwatres.2017.07.001.

725 Khaki, M., Ait-El-Fquih, B., Hoteit, I., Forootan, E., Awange, J., Kuhn, M., (2017c). A Two-
726 update Ensemble Kalman Filter for Land Hydrological Data Assimilation with an
727 Uncertain Constraint, *Journal of Hydrology*, Available online 25 October 2017, ISSN
728 0022-1694, <https://doi.org/10.1016/j.jhydrol.2017.10.032>.

729 Khaki, M., Forootan, E., Kuhn, M., Awange, J., Longuevergne, L., Wada, W., (2018), Efficient
730 Basin Scale Filtering of GRACE Satellite Products, In *Remote Sensing of Environment*,
731 Volume 204, 2018, Pages 76-93, ISSN 0034-4257,
732 <https://doi.org/10.1016/j.rse.2017.10.040>.

733 Kurnik, B., P. Barbosa, and J. Vogt (2011), Testing two different precipitation datasets to
734 compute the standerdised precipitation index over the Horn of Africa, *International*
735 *Journal of remote Sensing*, 32 (21), 5947-5964.

736 Kusche, J., Schmidt, R., Petrovic, S., Rietbroek, R. (2009), Decorrelated GRACEtime-variable
737 gravity solutions by GFZ, and their validation using a hydrological model.*Journal of*
738 *Geodesy*, 83, 903–913. <http://dx.doi.org/10.1007/s00190-0090308-3>.

739 Kusche, J., Eicker, A., Forootan, E., Springer, A., Longuevergne, L. (2016) Mapping
740 probabilities of extreme continental water storage changes from space gravimetry,
741 *Geophys. Res. Lett.*, 43, 8026–8034, doi:10.1002/2016GL069538.

742 Lau, K. and Shoo, P.J. (1988), Annual cycle, Quasi-Biennial Oscillation and Southern
743 Oscillation in global precipitation.*Journal of Geophysical Research*, 93, 10975-10988.

744 Lyon, B. (2014), Seasonal Drought in the Greater Horn of Africa and Its Recent Increase during
745 the March-May Long Rains, *Journal of Climate*, 27, 7953-7975.

746 Mpelasoka, F, J. L. Awange, R.MikoszGoncalves, (2017), Accounting for dynamics of mean
747 precipitation in drought projections: A case study of Brazil for the 2050 and 2070
748 periods, *Science of The Total Environment*, ISSN 0048-9697,
749 <https://doi.org/10.1016/j.scitotenv.2017.10.032>.

750 Naumann, G., E. Dutra, F. Pappenberger, F. Wetterhall, and J. V. Vogt (2014), Comparison of
751 drought indicators derived from multiple data sets over Africa, *Hydrology and*
752 *EarthSystem Sciences*, 18, 1625-1640.

753 Ndehedehe C, Awange J, Agutu N, Kuhn M, Heck B (2016) Understanding changes in
754 terrestrial water storage over West Africa between 2002 and 2014. *Advances in Water*
755 *Resources* 88: 211-230, doi: 10.1016/j.advwatres.2015.12.009.

756 Ndehedehe CE, Awange JL, Kuhn M, Agutu NO, Fukuda Y. (2017a) Climate teleconnections
757 influence on West Africa's terrestrial water storage. *Hydrological Processes*.31:3206–
758 3224. <https://doi.org/10.1002/hyp.11237>

759 Ndehedehe CE, Awange JL, Kuhn M, Agutu NO, Fukuda Y (2017b) Analysis of hydrological
760 variability over the Volta river basin using in-situ data and satellite observations. *Journal*
761 *of Hydrology: Regional Studies* 12: 88-110, doi: 10.1016/j.ejrh.2017.04.005.

762 Ndehedehe CE, Awange JL, Agutu NO, Okwuash O (2018) Changes in hydro-meteorological
763 conditions over tropical West Africa (1980-2015) and links to global climate. *Global*
764 *Planetary Change*, doi: 10.1016/j.gloplacha.2018.01.020.

765 Ni, S., Chen, J., Wilson, C.R. et al. (2018) Global Terrestrial Water Storage Changes and
766 Connections to ENSO Events. *Surv Geophys*, 39: 1, doi:10.1007/s10712-017-9421-7

767 Nicholson S.E, Kim, J.,1997: Relationship of ENSO to African rainfall. *Int. J. Climatol* 17:117–
768 135

769 Nicholson, S. E. and Kim, J. (1997), The relationship of the El Niño Southern Oscillation to
770 African rainfall, *Int. J. Climatol.*, 17, 117–135.

771 Nicholson S.E., Yin X., and Ba M. B. (2000), On the feasibility of using a lake water balance
772 model to infer rainfall: An example from Lake Victoria. *J. Hydrological Sciences*, 45,
773 75–96.

774 Nicholson S.E., (1996), A review of climate dynamics and climate variability in Eastern Africa.
775 The limnology, climatology and paleoclimatology of the Eastern Africa Lakes. Gordon
776 and Breach, New York, 57pp.

777 Ogallo, L.J. (1988), Relationships between seasonal rainfall in East Africa and the Southern
778 Oscillation', *Int. J. Climatol.*, 8, 31–43.

779 Omeny P.A., Ogallo, L.A., Okoola, R.A., Hendon, H., and Wheeler, M., (2008), East African
780 rainfall variability associated with the Madden-Julian Oscillation. *J. Kenya Meteorol.*
781 *Soc.*, 2(2) 105–114.

782 Omondi P, OgalloAwange, J, Ininda J, Forootan E. The influence of lowfrequency sea surface
783 temperature modes on delineated decadal rainfall zones in Eastern Africa region. *Adv.*
784 *Water Resour* 2013. [dx.doi.org/10.1016/j.advwatres.2013.01.001](https://doi.org/10.1016/j.advwatres.2013.01.001).

785 Phillips, T., Nerem, R.S., Fox-Kemper, B., Famiglietti, J.S., and Rajagopalan, B., (2012), The
786 influence of ENSO on global terrestrial water storage using GRACE, *GRL*, 39, L16705,
787 doi:10.1029/2012GL052495

788 Piper B. S., Plinston D.T., Sutcliffe, J. V., (1986), The water balance of Lake Victoria. *J.*
789 *Hydrological Sciences*, 31(1), 25-37

790 Preisendorfer R., (1988). *Principal component analysis in meteorology and oceanography.*
791 Elsevier: Amsterdam.

792 Reager J.T., and Famiglietti J.S. (2009), Global terrestrial water storage capacity and flood
793 potential using GRACE. *Geophysical Research Letters*, 36, L23402,1-6

794 Rietbroek, R., Brunnabend, S.E., Dahle, C., Kusche, J., Flechtner, F., Schröter, J., and
795 Timmermann, R. (2009), Changes in total ocean mass derived from GRACE, GPS, and
796 ocean modeling with weekly resolution. *Journal of Geophysical Research*, 114, C11004,
797 doi:10.1029/2009JC005449.

798 Saji N.H, Goswami, B.N., Vinayachandran, P.N., Yamagata, T.,1999: A dipole mode in the
799 tropical Indian Ocean. *Nature* 401:360–363
800 Stager J.C., Ruzmaikin A., Conway D., Verburg P., and Mason, P.J., (2007), Sunspots, El Nino,
801 and the levels of Lake Victoria, East Africa. *Journal of Geophysical Research*, VOL. 112,
802 D15106, doi:10.1029/2006JD008362
803 Swenson, S., and J. Wahr (2009), Monitoring the water balance of Lake Victoria, East Africa,
804 from space, *Journal of Hydrology*, 370, 163-176.
805 Tapley, B., Bettadpur, S., Ries, J., Thompson, P., and Watkins, M. (2004), GRACE
806 measurements of mass variability in the Earth system. *Science*,305,503-
807 505.<http://dx.doi.org/10.1126/science.1099192>
808 Thomas, A.C.; Reager, J.T.; Famiglietti, J.S.; Rodell, M. A (2014), GRACE-based water storage
809 deficit approach for hydrological drought characterization. *Geophys. Res. Lett.*, 41,
810 1537–1545.
811 Wahr, J., Molenaar, M., and Bryan, F. (1998), Time variability of the Earth's gravity field:
812 Hydrological and oceanic effects and their possible detection using GRACE. *Journal of*
813 *Geophysical Research*, 103 (B12), 30205-30229, doi:10.1029/98JB02844.
814 Wolter K., and Timlin, M.S., (2011), El Nino/Southern Oscillation behaviour since 1871 as
815 diagnosed in an extended multivariate ENSO index (MEI.ext). *International J.*
816 *Climatology*,31(7),1074-1087
817 Zhang, Z.; Chao, B.; Chen, J.; Wilson, C. (2015), Terrestrial water storage anomalies of Yangtze
818 River Basin droughts observed by GRACE and connections with ENSO. *Glob. Planet.*
819 *Chang.*, 126, 35–45.